Canadian Science Publishing | Biochemistry and Cell Biology

Circ_0000043 promotes breast cancer cell proliferation, migration, invasion and epithelial-mesenchymal transition via the miR-136/ Smad3 axis

Journal:	*Biochemistry and Cell Biology*
Manuscript ID	bcb-2020-0219.R1
Manuscript Type:	Article
Date Submitted by the Author:	15-Aug-2020
Complete List of Authors:	Leng, Xiaoling ; The Affiliated Tumor Hospital of Xinjiang Medical University Huang, Guofu ; The Fifth Affiliated Hospital of Xinjiang Medical University Ding, Jianbing ; Xinjiang Medical University, Ma, Fucheng ; The Affiliated Tumor Hospital of Xinjiang Medical University
Keyword:	Breast cancer, circ_0000043, miR-136, EMT
Is the invited manuscript for consideration in a Special Issue? :	Not applicable (regular submission)

Circ_0000043 promotes breast cancer cell proliferation, migration, invasion and epithelial-mesenchymal transition via the miR-136/ Smad3 axis

Running title: Circ_0000043, EMT, miR-136/Smad3

Xiaoling Leng[1], Guofu Huang[2], Jianbing Ding[3]*, Fucheng Ma[1]*

1. Department of Ultrasonography, The Affiliated Tumor Hospital of Xinjiang Medical University, Urumqi 830011, Xinjiang, P.R. China.
2. Department of Radio-Chemotherapy, The Fifth Affiliated Hospital of Xinjiang Medical University, Urumqi 830011, Xinjiang, P.R. China.
3. Department of Immunology, College of Basic Medicine, Xinjiang Medical University, Urumqi 830011, Xinjiang, P.R. China.

*** Corresponding Authors:**

Jianbing Ding: Xinjiang Medical University, 393 Xinyi Road, Urumqi, Xinjiang 830011, P.R. China. Email：bifuzhan8@163.com

Fucheng Ma: The Affiliated Tumor Hospital of Xinjiang Medical University, East Suzhou Road No.789, Urumqi, Xinjiang 830011, P.R. China. Email：ojxp795te@163.com

Funding

This work was supported by the National Natural Science Foundation of China (No. 81660496) and Xinjiang Youth Science and Technology Innovation Talent Training Project (No. 2017Q075).

Authors contribution

Conceived and designed the experiments: Jianbing Ding, Fucheng Ma;
Performed the experiments: Xiaoling Leng;
Statistical analysis: Xiaoling Leng, Guofu Huang;
Wrote the paper: Xiaoling Leng.
All authors read and approved the final manuscript.

Competing interests

The authors declare that they have no competing interests.

Ethics statement

Our study was approved by the Ethics Review Board of Xinjiang Medical University.

Data Availability Statement

The data used to support the findings of this study are available from the corresponding author upon request.

Abstract

Circular RNAs (circRNAs) are a type of tissue-specific RNA with more stable structure than linear RNAs, and its association with breast cancer (BC) is poorly understood. This study aimed at probing the biological effect of circ_0000043 in the progression of BC. In this study, expression of circ_0000043 in BC tissue samples was measured using quantitative real-time polymerase chain reaction (qRT-PCR). Immunohistochemistry (IHC) and Western blot were used to detect the expression of Smad family member 3 (Smad3). CCK-8, wound healing and Transwell assays were used to assess the effect of circ_0000043 in regulating BC cell proliferation, migration and invasion. Moreover, the binding relationships between circ_0000043 and miR-136, and miR-136 and Smad3 were detected by dual-luciferase reporter assay. Additionally, Western blot was used to detect the expressions of markers related to epithelial-mesenchymal transition (EMT), including E-cadherin, N-cadherin and vimentin. Our results showed that circ_0000043 expression was up-regulated in BC tissues and cell lines. Proliferation, migration, invasion and EMT of BC cells were significantly inhibited by circ_0000043 knockdown, and overexpression of circ_0000043 had the opposite effects. Additionally, circ_0000043 could up-regulate Smad3 expression by sponging miR-136. In conclusion, our study demonstrates that circ_0000043 can promote BC progression via regulating the miR-136/Smad3 axis.

Key words: circ_0000043, breast cancer, miR-136, Smad3

Introduction

Breast cancer (BC) is one of the most common tumors among women (Donepudi et al. 2014; Zeng et al. 2014). Its etiology is complex and related to genetic background, hormone levels, nutrition, environmental factors, etc. (Chen et al. 2016a). At present, there are still great challenges depriving BC patients of satisfactory clinical outcomes. Molecular targeted therapy becomes the focus of cancer research because of its low toxicity, few side effects and high efficiency. Therefore, it is particularly crucial to study the molecular mechanism of BC progression and seek novel therapy targets for BC.

Circular RNA (circRNA) is a class of endogenous non-coding RNAs widely found in the eukaryotic transcriptome. Unlike linear RNA, circRNA is not easy to be degraded and has a more stable structure. As a molecular sponge of miRNA or protein-binding RNA, circRNA can regulate gene expressions at the transcriptional or post-transcriptional level (Meng et al. 2017; Qu et al. 2015; Xu et al. 2018). CircRNA is regarded as a promising biomarker for disease diagnosis and therapy target for disease treatment, and figures prominently in the pathogenesis of human diseases, especially in cancers (Meng et al. 2017; Qu et al. 2015; Xu et al. 2018). However, the function of circRNA in BC has not been fully clarified.

MiRNA is a class of small non-coding RNA with 20-24 nucleotides in length. MiRNA inhibits translation through pairing with the 3'UTR of the target mRNA and participates in multiple biological activities, including proliferation, apoptosis, differentiation and so on (Gong et al. 2018; Jannot and Simard 2006; Lu et al. 2005). MiR-136 is linked to tumorigenesis and cancer progression. MiR-136 expression is reported to be up-regulated in human and mice lung cancer (Liu et al. 2010). In addition, miR-136 is highly expressed in the T-cell leukemia Jurkat cell line (Yu et al. 2006). Importantly, miR-136 expression is down-regulated in BC cancer tissues, and miR-136 can inhibit BC progression (Yan et al. 2016). However, the mechanism of miR-136 dysregulation in BC awaits further elucidation.

Belonging to Smad protein family, Smad family member 3 (Smad3) is a crucial transcription factor in the TGF-β/Smad signaling pathway. Besides, it is involved in various biological processes, including cell proliferation and differentiation, embryogenesis, angiogenesis, bone formation, tumorigenesis and epithelial-mesenchymal transition (EMT) (Huang et al. 2018; Wiercinska et al. 2011). It is reported that the expression of Smad3 is abnormally up-regulated/activated in BC. For example, TGF-β is found to strongly induce MMP2 and MMP9 in a Smad3-dependent manner in BC cells, and TGF-β-induced invasion of BC cells is reversed by knockdown of Smad3 (Wiercinska et al. 2011). The mutation of Smad3 phosphorylation site will impair the tumorigenesis and metastasis of BC cancer cells (Huang et al. 2018). However, little is known concerning the mechanism of its up-regulation and activation in BC.

There is little research about circRNA_0000043. Reportedly, circRNA_0000043 expression is up-regulated in endometrial cancer tissues and its overexpression can promote proliferation, migration and invasion of endometrial cancer cells (Zong et al. 2020). Interestingly, in lung adenocarcinoma cells, Smad3 is negatively regulated by miR-136 (Yang et al. 2013). Additionally, CircInteractome database indicates that circRNA_0000043 can probably interact with miR-136 and repress it. These data suggest that circRNA_0000043 may function as an oncogenic circRNA in BC by regulating miR-136 and Smad3. This study explored the regulatory effects of the circ_0000043/miR-136/Smad3 axis on the progression of BC, which might provide new targets for the treatments of BC.

Materials and Methods

Tissue samples collection

The cancer tissues of 40 BC patients who received surgery in the Affiliated Tumor Hospital of Xinjiang Medical University from May 2018 to May 2019 were randomly selected. None of the patients enrolled received neoadjuvant treatments prior to the surgery. The specimens of control group were from the paracancerous tissue of the same patients (at least 3 cm from the surgical

margin), and no cancer cells were found through postoperative pathological examination. All specimens were removed during the surgery and immediately stored in liquid nitrogen at -196 ℃ for the subsequent experiments. Our study was ratified by the Research Ethics Committee of the Affiliated Tumor Hospital of Xinjiang Medical University and the informed consent of all the patients was obtained.

Cell culture and cell transfection

Human normal breast epithelial cell line (MCF-10A) and BC cell lines (MDA-MB-231, MCF7 and ZR751) were purchased from the Institute of Biochemistry and Cell Biology of the Chinese Academy of Sciences (Shanghai, China). These cells were cultured in RPMI-1640 medium (Gibco, Grand Island, NY, USA) containing 10 % fetal bovine serum (FBS, HyClone, Logan, UT, USA), 100 U/mL penicillin and 0.1 mg/mL streptomycin (Sigma, St. Louis, MO, USA). The cells were cultured in an incubator with 5 % of CO_2 (volume fraction) at 37 ℃.

pcDNA empty vector (NC), pcDNA-circ_0000043, shRNA normal control (sh-NC), shRNA against circ_0000043 (sh-circ_0000043), miRNA control (miR-NC), miR-136 mimics and miR-136 inhibitors were designed and provided by GenePharma Co., Ltd. (Shanghai, China). ZR751 and MDA-MB-231 cells were inoculated on 24-well cell culture plates with 3×10^5 cells/well. Lipofectamine®3000 (Invitrogen, New York, CA, USA) and plasmids or oligonucleotides mentioned above were mixed, and cells were cultured in RPMI-1640 medium without FBS for 24 h. Then the mixture was added to the medium. After 24 h, the medium was changed to complete medium, and quantitative real-time polymerase chain reaction (qRT-PCR) was used to detect transfection efficiency after 36 h of culture.

RNA extraction and qRT-PCR

Total RNA of tissue or cell was extracted using TRIzol reagent (Invitrogen, New York, CA, USA). Nanodrop-spectrophotometer was used to detect RNA concentration and purity. According to the manufacturer's instruction, PrimeScript-RT Kit (Madison Biotechnology Co., Ltd, Madison, WI, USA) was used to synthesize the complementary DNA (cDNA), and then, with cDNA as the template, qRT-PCR was performed using SYBR® Premix-Ex-TaqTM (Takara, Osaka, Japan) on ABI 7300 Real-time PCR System (Applied Biosystems, Foster City, CA, USA). GAPDH was the

internal reference of circ_0000043 and Smad3, and U6 was the internal reference of miR-136. The primers were designed, synthesized and provided by RiboBio Co., Ltd. (Guangzhou, China). The primers for qRT-PCR were shown in Table 1.

Immunohistochemistry (IHC)

BC tissues and normal tissues were fixed in 10 % formaldehyde and embedded in paraffin. After that, the paraffin-embedded tissues were cut into 4-μm-thick sections. After dewaxing, rehydration and antigen recovery, the sections were incubated with anti-Smad3 antibody (ab40854, 1: 500, Abcam, Shanghai, China) at 4 °C for 12 h, and then washed with PBS, followed by the incubation with biotin-linked antiserum for 1 h at room temperature. Next, the sections were washed again and stained with DAB (Beyotime, Shanghai, China) for 1 min. Then the sections were stained with hematoxylin for 1 min, observed and then scored by two independent pathologists.

Cell counting kit-8 (CCK-8) assay

ZR751 and MDA-MB-231 cells from each group were harvested and inoculated into 96-well plates with a density of 2×10^3 / well. After that, the culture plates were put into an incubator. After 12 h, 10 μL CCK-8 solution (Beyotime, Shanghai, China) was added to each well, with which the cells were incubated for 4 h. Subsequently, the absorbance of cells at 450 nm was measured by a microplate reader. The same operation was repeated at 24 h, 48 h, 72 h and 96 h after inoculation, respectively, and after that, the proliferation curve was plotted.

Wound healing assay

ZR751 and MDA-MB-231 cells in logarithmic growth phase were collected and inoculated in 24-well plates at a density of 2.5×10^5 cells / well and cultured in an incubator with 5 % CO_2 at 37 ℃. After the cells fully covered the bottom of the wells, the medium was discarded, and cells were rinsed with PBS twice. 200 μL pipette was employed to make a scratch. After that, cells were rinsed with PBS again, and serum-free medium was loaded into each well. The scratch was observed and photographed under a microscope. Then cell culture was continued, and the scratch was observed and photographed again after 24 h.

Transwell assay

The ZR751 and MDA-MB-231 cells were harvested and resuspended with serum-free RPMI-1640 medium (Gibco, Grand Island, NY, USA), and the cell density was modulated to 1×10^5 cells/ml. Then 200 μL cell suspension and RPMI-1640 medium containing 10 % FBS were added into the upper compartment and the lower compartment of each Transwell chamber (8 μm pore diameter, Corning, Shanghai, China) coated with Matrigel (BD Biosciences, Franklin Lakes, NJ, USA), respectively, before the cells were cultured for 12 h. Then, the Transwell chamber was removed and the non-invaded cells on the membrane were wiped off with a cotton swab. The invaded cells were fixed with 4 % paraformaldehyde and stained with crystal violet. Finally, under the microscope, five fields of view on the Transwell membrane were randomly selected to calculate the number of cells passing through the membrane, so as to evaluate the cell invasive ability.

Dual-luciferase reporter gene assay

In brief, wild type (WT) and mutant (MUT) luciferase reporter vectors (circ_0000043-WT, circ_0000043-MUT, Smad3-WT and Smad3-MUT) were co-transfected into MDA-MB-231 cells with miR-136 mimics or miR-NC using lipofectamine®3000 (Invitrogen, New York, CA, USA). After 48 h, luciferase activity in each group was determined with Dual-Luciferase Reporter Assay System (Promega, Madison, WI, USA) in compliance with the manufacturer's protocols.

RNA immunoprecipitation (RIP) assay.

RIP assay was performed using the Magna RIP™ RNA Binding Protein Immunoprecipitation kit (Millipore, Billerica, MA, USA) in line with manufacturer's instructions. In brief, MDA-MB-231 cells were collected and lysed in cleavage buffer. Next, 200 μL cell lysate was incubated with anti-Ago2 antibody or rabbit IgG-coupled magnetic beads at 4 ℃ overnight. The complex containing magnetic beads/antibody was washed and then resuspended using RIP washing buffer. After being treated with protease K buffer, total RNA was extracted from the immunoprecipitate, and qRT-PCR was performed to detect the expression levels of circ_0000043 and miR-136.

Western blot

RIPA lysate (Beyotime Biotcchnology, Shanghai, China) was used to extract the total protein of

the ZR751 and MDA-MB-231 cells, and the BCA protein detection kit (Pierce, Rockford, IL, USA) was used to detect the protein concentration. Sodium dodecyl sulfate polyacrylamide gel electrophoresis (SDS-PAGE) was utilized to separate the protein, and the protein was then electrophoretically transferred to polyvinylidene fluoride (PVDF) membrane (Millipore, Bedford, MA, USA). Next, the membrane was blocked at room temperature with 5 % skim milk for 2 h at room temperature, and then the primary antibodies, including anti-Smad3 antibody (ab40854, 1:1000, Abcam, Shanghai, China), anti-E Cadherin antibody (ab1416, 1:1000, Abcam, Shanghai, China), anti-N-Cadherin antibody (ab18203, 1:1000, Abcam, Shanghai, China), anti-Vimentin antibody (ab8978, 1:1000, Abcam, Shanghai, China) and anti-GAPDH antibody (ab181602, 1:2000, Abcam, Shanghai, China), were added to incubate the membrane at 4 ℃ for 12 h. After that, the membrane was washed, and HRP-labeled secondary antibody (ab205718, 1:2000, Abcam, Shanghai, China) was added, with which the membrane was incubated at room temperature for 1 h. Moreover, ECL chemiluminescence kit (Millipore, Bedford, MA, USA) was used for band development.

Statistical Methods

SPSS 17.0 statistical software (SPSS Inc., Chicago, IL, USA) was employed for data analysis. The measurement data were expressed as mean ± standard deviation (x ± s). Comparison between the two groups was tested by *t*-test. The counting data in two groups were compared by $\chi 2$ test. The difference was statistically significant with $P < 0.05$.

Results

Circ_0000043 was highly expressed in BC tissues and cells.

First of all, we investigated the expression of circ_0000043 in BC tissues and cells. The results of qRT-PCR showed that compared with in normal breast tissues and MCF-10A cells, the expression of circ_0000043 in BC tissues and cell lines (MDA-MB-231, MCF7 and ZR751) was increased (Figure 1A-B). In addition, we analyzed the correlation between circ_0000043 expression and pathological characteristics. The data indicated that high expression of circ_0000043 was remarkably associated with lymph node metastasis and poor differentiation of tumor tissues (Table 2). These results implied that high expression of circ_0000043 was related to poor prognosis of

patients.

Effects of circ_0000043 on BC cell proliferation, migration, invasion and epithelial-mesenchymal transition (EMT).

Next, we pinpointed the biological function of circ_0000043 in BC. Circ_0000043 overexpression and knockdown cell lines were constructed with ZR751 and MDA-MB-231 cell lines, respectively, and qRT-PCR proved that the transfection was successful. (Figure 2A-B). CCK-8 assay results depicted that the proliferation of ZR751 cells was up-regulated after circ_0000043 overexpression, and circ_0000043 knockdown repressed the proliferation of MDA-MB-231 cells (Figure 2C-D). Wound healing and Transwell assays manifested that the migration and invasion abilities of ZR751 cells were markedly up-regulated after overexpression of circ_0000043, while knocking down circ_ 0000043 had the opposite effects in MDA-MB-231. (Figure 2E-F). Western blot results unveiled that compared with the control group, the expression of the epithelial cell marker E-cadherin in ZR751 cells with circ_0000043 overexpression was markedly reduced, while the expressions of mesenchymal cell markers N-cadherin and Vimentin were remarkably increased; conversely, knocking down circ_0000043 in MDA-MB-231 had reversed effects (Figure 2G). These results revealed that circ_0000043 could serve as a cancer-promoting circRNA to promote BC cell proliferation, local migration and invasion and EMT process.

Circ_0000043 directly interacted with miR-136.

Bioinformatics database CircInteractome suggested that circ_0000043 contained a potential binding site for miR-136 (Figure 3A). Dual-luciferase reporter assay was performed to verify the relationship between them, and miR-136 mimics or the negative controls were co-transfected into MDA-MB-231 cells, the findings of which demonstrated that miR-136 mimics could dramatically reduce the luciferase activity of circ_0000043-WT reporter, but had no significant effect on the luciferase activity of circ_0000043-MUT reporter (Figure 3B). This result ascertained the specific base paring relationship between circ_0000043 and miR-136. Moreover, we performed RIP experiment, and MDA-MB-231 cells were transfected with miR-136 mimics or the control miRNAs. The results showed that compared with the control group, anti-Ago2 antibody enriched more circ_0000043 (Figure 3C), which implied a direct interaction between miR-136 and

circ_0000043. Additionally, qRT-PCR experiments indicated that after overexpression and knockdown of circ_0000043, the expression of miR-136 in BC cell lines was down-regulated and up-regulated, respectively (Figure 3D-E). These results betokened that circ_0000043 could target miR-136 and inhibit its expression.

Smad3 was a downstream target of miR-136

In order to elaborate on the downstream molecular mechanism of miR-136, we screened candidate targets of miR-136 with TargetScan. It was suggested that miR-136 could probably bind to the 3'UTR of Smad3 mRNA (Figure 4A). The dual-luciferase reporter assay in MDA-MB-231 cells manifested that miR-136 could remarkably down-regulate the luciferase activity of Smad3 3'UTR-WT reporter, but had no remarkable effect on that of Smad3 3'UTR-MUT reporter (Figure 4B). Furthermore, Western blot assay was utilized to detect the relationship between Smad3 and miR-136 or circ_0000043 in BC cell lines. The results uncovered that after the transfection of miR-136 mimics and inhibitors, the expression level of Smad3 in BC cells was down-regulated and up-regulated, respectively (Figure 4C). Additionally, the expressions of Smad3 in ZR751 with circ_0000043 overexpression and MDA-MB-231 cells with circ_0000043 knockdown were up-regulated and down-regulated, respectively (Figure 4D). These results unearthed that in BC cells, Smad3 was a target gene of miR-136 and was positively regulated by circ_0000043.

Circ_0000043 regulated BC cell proliferation, migration, invasion and EMT through miR-136/Smad3 axis.

Next, we transfected miR-136 mimics into ZR751 cells with high expression of circ_0000043, and the transfection efficiency was confirmed by qRT-PCR (Figure 5A-C). The results of functional experiments displayed that the proliferation, migration and invasion of ZR751 cells in circ-0000043 / miR-136 group were significantly inhibited than those in circ-0000043 / miR-NC group (Figure 5D-F). In addition, compared with in the circ_0000043 / miR-NC group, the expression of E-cadherin in the circ_0000043 / miR-136 group was markedly enhanced, while the expressions of N-cadherin and Vimentin were decreased dramatically. (Figure 5G). These results confirmed that miR-136 could partially reverse the function of circ_0000043 in promoting BC cell proliferation, migration, invasion and EMT, which further illustrated that circ_0000043 could

promote the proliferation, local migration and invasion and EMT of BC cells by regulating the miR-136/Smad3 axis.

The correlations among circ_0000043, Smad3 and miR-136 in BC tissues.

At last, we used Pearson's correlation analysis to detect the correlations among circ_0000043, Smad3 mRNA and miR-136 in BC tissue samples, the results of which demonstrated that in BC tissues, there were negative correlations between expressions of miR-136 and circ_0000043, and miR-136 and Smad3 mRNA; there was a positive correlation between the expressions of circ_0000043 and Smad3 mRNA (Figure 6A-C). The results of immunohistochemistry further authenticated that high expression level of Smad3 protein in BC tissues was associated with high expression of circ_0000043 (Figure 6D). These results further validated that there were regulatory relationships among circ_0000043, miR-136 and Smad3 in BC.

Discussion

Accumulating studies report that abnormal expressions of circRNAs are involved in the progression of tumors. For example, circ_0000064 expression is up-regulated in lung cancer tissues and cells, and its high expression is related to adverse clinical characteristics, including higher T stage and lymph node metastasis; knockdown of circ_0000064 represses the malignant phenotypes of lung cancer cells (Luo et al. 2017); circPTK2 inhibits the expression of TIF1γ in non-small cell lung cancer, thereby blocking the TGF-β-induced EMT process (Wang et al. 2018). Importantly, multiple circRNAs are found to be abnormally expressed in BC tissues, and they are proved to be crucial modulator during BC progression. A study demonstrates that circ-Foxo3 is underexpressed in BC tissues and cell, and its ectopic expression induces stress-induced apoptosis and reduces proliferation of cancer cells (Du et al. 2017); circ-Dnmt1 interacts with both p53 and AUF1, and promotes the nuclear translocation of them, which triggers autophagy to promote cancer progression (Du et al. 2018); additionally, circANKS1B up-regulates the expression of TGF-β1, thus activating the TGF-β1/Smad signaling pathway and promoting EMT (Zeng et al. 2018). Interestingly, circ_0000043 was found to promote endometrial cancer cell proliferation and migration via targeting miR-136/NOTCH3 pathway (Zong et al. 2020). In this study, it was

observed that the expression of circ_0000043 was significantly up-regulated in BC tissues and cell lines; high expression of circ_0000043 was associated with adverse pathological indicators of the patients; overexpression of circ_0000043 could promote BC cell proliferation, local migration and invasion and EMT, while knocking down circ_0000043 functioned oppositely. For the first time, circ_0000043 was identified as an oncogenic circRNA in BC in this study. These data also suggested that circ_0000043 was a potential biomarker and therapy target for BC.

Multiple miRNAs are abnormally expressed in many tumors, and they can function as a tumor promoter or suppressor (Caldas and Brenton 2005). Even though miR-136 expression is reported to be up-regulated and function as an oncogenic miRNA in several cancers such as leukemia and lung cancer, in most cancers, miR-136 is well known as a tumor suppressor (Liu et al. 2010; Yu et al. 2006). For instance, in esophageal squamous cell carcinoma, it induces the apoptosis of cancer cells and increases the radiosensitivity by repressing mucin 1 (Huang et al. 2019). In hepatocellular carcinoma, miR-136 inhibits proliferation and migration of cancer cells by targeting cyclooxygenase 2 (Abulizi et al. 2019). In osteosarcoma, decreased miR-136 expression is significantly associated with higher Enneking staging and distant metastasis (Chu et al. 2019). Some researches confirm that miR-136 is a tumor suppressor in BC. In triple-negative breast cancer, it suppresses tumor invasion and metastasis by down-regulating RAS protein activator like 2 (Yan et al. 2016). Additionally, it is reported that down-regulation of miR-136 expression in BC can activate the Wnt / β-catenin signaling pathway, thereby promoting cancer progression (Huan et al. 2017). Our results suggested that miR-136 mimics could partially reverse the effect of circ_0000043 on the progression of BC, which is consistent with previous reports (Huan et al. 2017; Yan et al. 2016). Additionally, in this work, it was illustrated that Smad3 was a target gene of miR-136 in BC, which further clarified the mechanism of miR-136 in cancer biology.

Smad3 is a crucial mediator in multiple signaling pathways in cancer biology (Chen et al. 2016b; Derynck et al. 1996). In breast cancer, CCL2/CCR2 axis coordinates the survival and movement of BC cells through Smad3 and p42/44MAPK-dependent mechanisms (Fang et al. 2012).

Transcriptional activation of EGFR induced by TGF-β in BC is mediated by Smad3 and ERK/Sp1 signaling pathways (Zhao et al. 2018). Additionally, a recent study indicates that HDAC8 cooperates with Smad3/4 complex to suppress SIRT7 and promote BC progression (Tang et al. 2020). In our work, a novel mechanism by which Smad3 expression is up-regulated was presented. It was demonstrated that Smad3 was negatively regulated by miR-136, but positively regulated by circ_0000043.

It should be noted that this study has several limitations. Above all, *in vivo* experiments, such as nude mice tumorigenesis assay, are required to further verify the oncogenic function of circ_0000043. In addition, more patients should be included to perform survival analysis based on the expression of circ_0000043, and other downstream targets of circ_0000043 remain to be screened and identified. All in all, this work shows that circ_0000043 expression is up-regulated in BC tissues and cells, and circ_0000043 can promote the proliferation, local migration and invasion and EMT of BC cells, and circ_0000043 mainly plays its role by regulating miR-136/Smad3 axis. Our findings suggest that circ_0000043 is a potential biomarker and therapeutic target for BC.

References

Abulizi, R., Li, B., and Zhang, C.G. 2019. Circ_0071662, a novel tumor biomarker, suppresses bladder cancer cell proliferation and invasion by sponging miR-146b-3p. Oncology research. doi:10.3727/096504019x15740729375088.

Caldas, C., and Brenton, J.D. 2005. Sizing up miRNAs as cancer genes. Nature medicine **11**(7): 712-714. doi:10.1038/nm0705-712.

Chen, W., Zheng, R., Baade, P.D., Zhang, S., Zeng, H., Bray, F., et al. 2016a. Cancer statistics in China, 2015. CA Cancer J Clin **66**(2): 115-132. doi:10.3322/caac.21338.

Chen, X., Cao, X., Sun, X., Lei, R., Chen, P., Zhao, Y., et al. 2016b. Bcl-3 regulates TGFβ signaling by stabilizing Smad3 during breast cancer pulmonary metastasis. Cell death & disease **7**(12): e2508. doi:10.1038/cddis.2016.405.

Chu, Y., Hu, X., Wang, G., Wang, Z., and Wang, Y. 2019. Downregulation of miR-136 promotes the progression of osteosarcoma and is associated with the prognosis of patients with osteosarcoma. Oncology letters **17**(6): 5210-5218. doi:10.3892/ol.2019.10203.

Derynck, R., Gelbart, W.M., Harland, R.M., Heldin, C.H., Kern, S.E., Massagué, J., et al. 1996. Nomenclature: vertebrate mediators of TGFbeta family signals. Cell **87**(2): 173. doi:10.1016/s0092-8674(00)81335-5.

Donepudi, M.S., Kondapalli, K., Amos, S.J., and Venkanteshan, P. 2014. Breast cancer statistics and markers. Journal of cancer research and therapeutics **10**(3): 506-511. doi:10.4103/0973-1482.137927.

Du, W.W., Fang, L., Yang, W., Wu, N., Awan, F.M., Yang, Z., et al. 2017. Induction of tumor apoptosis through a circular RNA enhancing Foxo3 activity. Cell Death Differ **24**(2): 357-370. doi:10.1038/cdd.2016.133.

Du, W.W., Yang, W., Li, X., Awan, F.M., Yang, Z., Fang, L., et al. 2018. A circular RNA circ-DNMT1 enhances breast cancer progression by activating autophagy. Oncogene **37**(44): 5829-5842. doi:10.1038/s41388-018-0369-y.

Fang, W.B., Jokar, I., Zou, A., Lambert, D., Dendukuri, P., and Cheng, N. 2012. CCL2/CCR2 chemokine signaling coordinates survival and motility of breast cancer cells through Smad3 protein- and p42/44 mitogen-activated protein kinase (MAPK)-dependent mechanisms. J Biol Chem **287**(43): 36593-36608. doi:10.1074/jbc.M112.365999.

Gong, P., Qiao, F., Wu, H., Cui, H., Li, Y., Zheng, Y., et al. 2018. LncRNA UCA1 promotes tumor metastasis by inducing miR-203/ZEB2 axis in gastric cancer. Cell death & disease **9**(12): 1158. doi:10.1038/s41419-018-1170-0.

Huan, J., Xing, L., Lin, Q., Xui, H., and Qin, X. 2017. Long noncoding RNA CRNDE activates Wnt/β-catenin signaling pathway through acting as a molecular sponge of microRNA-136 in human breast cancer. American journal of translational research **9**(4): 1977-1989.

Huang, C.C., Huang, M.S., Chung, H.J., Chiu, S.Y., Yadav, P., Lin, Y., et al. 2018. Impaired mammary tumor formation and metastasis by the point mutation of a Smad3 linker phosphorylation site. Biochimica et biophysica acta. Molecular basis of disease **1864**(11): 3664-3671. doi:10.1016/j.bbadis.2018.08.031.

Huang, H.Z., Yin, Y.F., Wan, W.J., Xia, D., Wang, R., and Shen, X.M. 2019. Up-regulation of

microRNA-136 induces apoptosis and radiosensitivity of esophageal squamous cell carcinoma cells by inhibiting the expression of MUC1. Experimental and molecular pathology **110**: 104278. doi:10.1016/j.yexmp.2019.104278.

Jannot, G., and Simard, M.J. 2006. Tumour-related microRNAs functions in Caenorhabditis elegans. Oncogene **25**(46): 6197-6201. doi:10.1038/sj.onc.1209921.

Liu, X., Sempere, L.F., Ouyang, H., Memoli, V.A., Andrew, A.S., Luo, Y., et al. 2010. MicroRNA-31 functions as an oncogenic microRNA in mouse and human lung cancer cells by repressing specific tumor suppressors. J Clin Invest **120**(4): 1298-1309. doi:10.1172/jci39566.

Lu, J., Getz, G., Miska, E.A., Alvarez-Saavedra, E., Lamb, J., Peck, D., et al. 2005. MicroRNA expression profiles classify human cancers. Nature **435**(7043): 834-838. doi:10.1038/nature03702.

Luo, Y.H., Zhu, X.Z., Huang, K.W., Zhang, Q., Fan, Y.X., Yan, P.W., et al. 2017. Emerging roles of circular RNA hsa_circ_0000064 in the proliferation and metastasis of lung cancer. Biomed Pharmacother **96**: 892-898. doi:10.1016/j.biopha.2017.12.015.

Meng, S., Zhou, H., Feng, Z., Xu, Z., Tang, Y., Li, P., et al. 2017. CircRNA: functions and properties of a novel potential biomarker for cancer. Mol Cancer **16**(1): 94. doi:10.1186/s12943-017-0663-2.

Qu, S., Yang, X., Li, X., Wang, J., Gao, Y., Shang, R., et al. 2015. Circular RNA: A new star of noncoding RNAs. Cancer Lett **365**(2): 141-148. doi:10.1016/j.canlet.2015.06.003.

Tang, X., Li, G., Su, F., Cai, Y., Shi, L., Meng, Y., et al. 2020. HDAC8 cooperates with SMAD3/4 complex to suppress SIRT7 and promote cell survival and migration. Nucleic acids research **48**(6): 2912-2923. doi:10.1093/nar/gkaa039.

Wang, L., Tong, X., Zhou, Z., Wang, S., Lei, Z., Zhang, T., et al. 2018. Circular RNA hsa_circ_0008305 (circPTK2) inhibits TGF-β-induced epithelial-mesenchymal transition and metastasis by controlling TIF1γ in non-small cell lung cancer. Mol Cancer **17**(1): 140. doi:10.1186/s12943-018-0889-7.

Wiercinska, E., Naber, H.P., Pardali, E., van der Pluijm, G., van Dam, H., and ten Dijke, P. 2011. The TGF-β/Smad pathway induces breast cancer cell invasion through the up-regulation of matrix metalloproteinase 2 and 9 in a spheroid invasion model system. Breast cancer

research and treatment **128**(3): 657-666. doi:10.1007/s10549-010-1147-x.

Xu, Z., Yan, Y., Zeng, S., Dai, S., Chen, X., Wei, J., et al. 2018. Circular RNAs: clinical relevance in cancer. Oncotarget **9**(1): 1444-1460. doi:10.18632/oncotarget.22846.

Yan, M., Li, X., Tong, D., Han, C., Zhao, R., He, Y., et al. 2016. miR-136 suppresses tumor invasion and metastasis by targeting RASAL2 in triple-negative breast cancer. Oncol Rep **36**(1): 65-71. doi:10.3892/or.2016.4767.

Yang, Y., Liu, L., Cai, J., Wu, J., Guan, H., Zhu, X., et al. 2013. Targeting Smad2 and Smad3 by miR-136 suppresses metastasis-associated traits of lung adenocarcinoma cells. Oncol Res **21**(6): 345-352. doi:10.3727/096504014x14024160459285.

Yu, J., Wang, F., Yang, G.H., Wang, F.L., Ma, Y.N., Du, Z.W., et al. 2006. Human microRNA clusters: genomic organization and expression profile in leukemia cell lines. Biochem Biophys Res Commun **349**(1): 59-68. doi:10.1016/j.bbrc.2006.07.207.

Zeng, H., Zheng, R., Zhang, S., Zou, X., and Chen, W. 2014. Female breast cancer statistics of 2010 in China: estimates based on data from 145 population-based cancer registries. Journal of thoracic disease **6**(5): 466-470. doi:10.3978/j.issn.2072-1439.2014.03.03.

Zeng, K., He, B., Yang, B.B., Xu, T., Chen, X., Xu, M., et al. 2018. The pro-metastasis effect of circANKS1B in breast cancer. Mol Cancer **17**(1): 160. doi:10.1186/s12943-018-0914-x.

Zhao, Y., Ma, J., Fan, Y., Wang, Z., Tian, R., Ji, W., et al. 2018. TGF-β transactivates EGFR and facilitates breast cancer migration and invasion through canonical Smad3 and ERK/Sp1 signaling pathways. Mol Oncol **12**(3): 305-321. doi:10.1002/1878-0261.12162.

Zong, Z. H., Liu, Y., Chen, S., and Zhao, Y. 2020. Circ_PUM1 promotes the development of endometrial cancer by targeting the miR-136/NOTCH3 pathway. Journal of cellular and molecular medicine. **24**(7): 4127–4135. doi:10.1111/jcmm.15069

Tab 1 Primers used for qRT-PCR

Genes	Primers
miR-136	Forward: 5’-GCGCACTCCATTTGTTTTGAT-3’
	Reverse: 5'-GTGCAGGGTCCGAGGT-3'
U6	Forward: 5’-AAAGCAAATCATCGGACGACC-3’

	Reverse: 5’-GTACAACACATTGTTTCCTCGGA-3’
circ_0000043	Forward: 5’- TATTCAGGCACGCAGGTACC-3’
	Reverse: 5’-TCACTGTCTGCATCCCTTGG-3’
Smad3	Forward 5’-CTCCAAACCTATCCCCGAAT-3’
	Reverse 5’-CCTGTTGACATTGGAGAGCA-3’
GAPDH	Forward: 5'-TGTGGGCATCAATGGATTTGG-3'
	Reverse: 5'-ACACCATGTATTCCGGGTCAAT-3'

Tab 2 Association between circ_0000043 expression and clinicopathological characteristics

Characteristic	Group	n	circ_0000043		*P* value
			Low (n=20)	High (n=20)	
Age(years)	≤50	18	6	12	0.0736
	＞50	22	14	8	
Tumor size(cm)	≤2	15	6	9	0.3272
	＞2	25	14	11	
Differentiation grade	G1+2	17	14	3	0.0004***
	G3	23	6	17	
Histological type	Ductal	13	5	8	0.3112
	Lobular	27	15	12	
ER status	Negative	25	14	11	0.3272
	Positive	15	6	9	
PR status	Negative	24	13	11	0.5186
	Positive	16	7	9	
HER-2 status	Negative	16	6	10	0.302
	Positive	24	14	10	
Lymph node metastasis	Absent	16	14	2	0.0001***
	Present	24	6	18	

Notes: *** presents $P < 0.001$

469

470

471

Figure 1: Circ_0000043 was highly expressed in BC tissues and cells.

A-B: qRT-PCR demonstrated that the expression of circ_0000043 in BC tissues and cells (MCF-10A, MDA-MB-231, MCF7 and ZR751) was significantly upregulated..

$P < 0.05$ denoted by *, $P < 0.01$ denoted by **, $P < 0.001$ denoted by ***.

Figure 2: Effects of overexpression and knockdown of circ_0000043 on BC cell proliferation, metastasis, and EMT.

A-B: qRT-PCR was used to detect the expression of circ_0000043 in ZR751 and MDA-MB-231 cells after over-expression and knockdown of circ_0000043. C-D: CCK-8 assay indicated that overexpression of circ_0000043 promoted proliferation of ZR751 cells and knockdown of circ_0000043 inhibited proliferation of MDA-MB-231 cells. E-F: Wound healing assay and Transwell assay indicated that overexpression of circ_0000043 promoted migration and invasion of ZR751 cells and knockdown of circ_0000043 in MDA-MB-231 cells functioned oppositely. G: Western blot data suggested circ_0000043 promoted N-cadherin and Vimentin expressions but inhibited E-cadherin expression.

$P < 0.05$ denoted by *, $P < 0.01$ denoted by **, $P < 0.001$ denoted by ***.

Figure 3: Circ_0000043 had a targeting relationship with miR-136.

A: Circ_0000043 contained a potential binding site for miR-136. B: The targeting relationship between circ 0000043 and miR-136 was validated by dual luciferase report assay with MDA-MB-231 cells. C: In MDA-MB-231 cells, RIP experiment found that circ_0000043 directly interacted with miR-136. D-E: qRT-PCR demonstrated that overexpression of circ_0000043 in ZR751 cells inhibited miR-136 expression and knockdown of circ_0000043 in MDA-MB-231 cells promoted miR-136 expression.

$P > 0.05$ denoted by ns, $P < 0.01$ denoted by **, $P < 0.001$ denoted by ***.

Figure 4: Smad3 was a downstream target of miR-136.

A: The 3'UTR of Smad3 was found to contain a potential binding site for miR-136. B: Dual luciferase report assay was used to detect the targeting relationship between miR-136 and Smad3 in MDA-MB-231 cells. C-D: Western blot assay data showed that miR-136 inhibited SMAD3 expression but circ_0000043 promoted SMAD3 expression.

$P > 0.05$ denoted by ns, $P < 0.01$ denoted by **, $P < 0.001$ denoted by *** .

Figure 5: Circ_0000043 promoted BC cell proliferation, metastasis, and EMT through miR-136 / Smad3 axis.

A-C: After miR-136 mimics were transfected into ZR751 cells overexpressing circ_0000043, the expressions of circ_0000043, miR-136 and Smad3 mRNA were detected by RT-PCR. D: CCK-8 assay indicated that miR-136 reversed the effect of circ_0000043 on proliferation of ZR751 cells. E-F: Wound healing and Transwell assays suggested that miR-136 reversed the effects of circ_0000043 on migration and invasion of ZR751 cells. G: Western blot assay demonstrated that miR-136 reversed the effect of circ_0000043 on EMT of ZR751 cells.

$P < 0.05$ indicated by *, $P < 0.01$ indicated by **, $P < 0.001$ indicated by ***. In figure D, , $P < 0.05$ indicated by *, $P < 0.01$ indicated by ** (vs Vector group); $P < 0.05$ indicated by # (vs circ_0000043 / miR-NC group)

Figure 6: The correlation of circ_0000043, Smad3 and miR-136 in BC tissues.

A-C: The negative correlations between miR-136 and circ_0000043, miR-135 and SMAD3 mRNA, and the positive correlation between circ_0000043 and SMAD3 mRNA in BC tissues were found by Pearson's correlation analysis. D: Immunohistochemical staining was performed, and chi-square test indicated the significant positive correlation between Smad3 protein expression and circ_0000043 expression in BC samples.

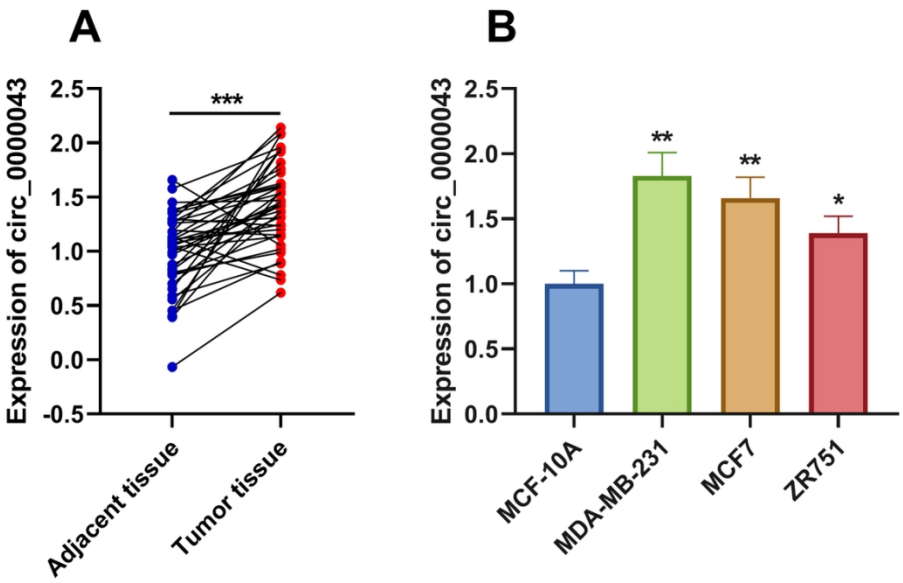

Figure 1: Circ_0000043 was highly expressed in BC tissues and cells.
A-B: qRT-PCR demonstrated that the expression of circ_0000043 in BC tissues and cells (MCF-10A, MDA-MB-231, MCF7 and ZR751) was significantly upregulated..
P < 0.05 denoted by *, P < 0.01 denoted by **, P < 0.001 denoted by ***.

110x73mm (300 x 300 DPI)

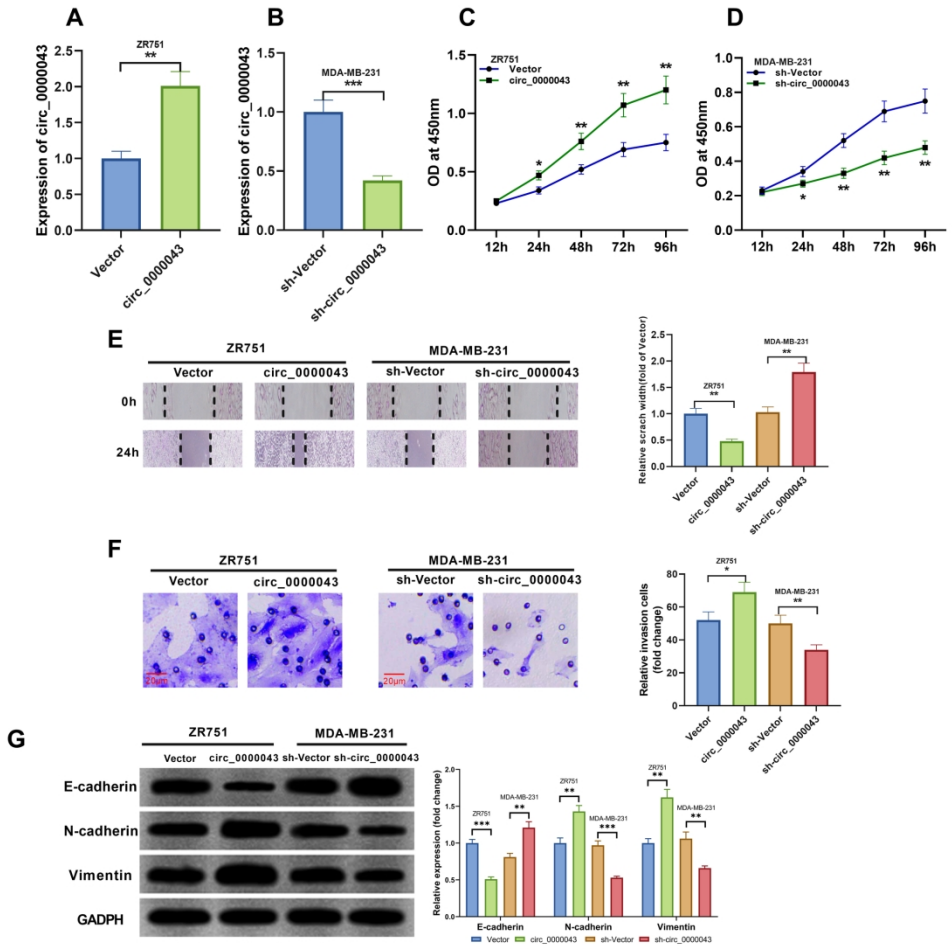

Figure 2: Effects of overexpression and knockdown of circ_0000043 on BC cell proliferation, metastasis, and EMT.
A-B: qRT-PCR was used to detect the expression of circ_0000043 in ZR751 and MDA-MB-231 cells after over-expression and knockdown of circ_0000043. C-D: CCK-8 assay indicated that overexpression of circ_0000043 promoted proliferation of ZR751 cells and knockdown of circ_0000043 inhibited proliferation of MDA-MB-231 cells. E-F: Wound healing assay and Transwell assay indicated that overexpression of circ_0000043 promoted migration and invasion of ZR751 cells and knockdown of circ_0000043 in MDA-MB-231 cells functioned oppositely. G: Western blot data suggested circ_0000043 promoted N-cadherin and Vimentin expressions but inhibited E-cadherin expression.
$P < 0.05$ denoted by *, $P < 0.01$ denoted by **, $P < 0.001$ denoted by ***.

200x197mm (300 x 300 DPI)

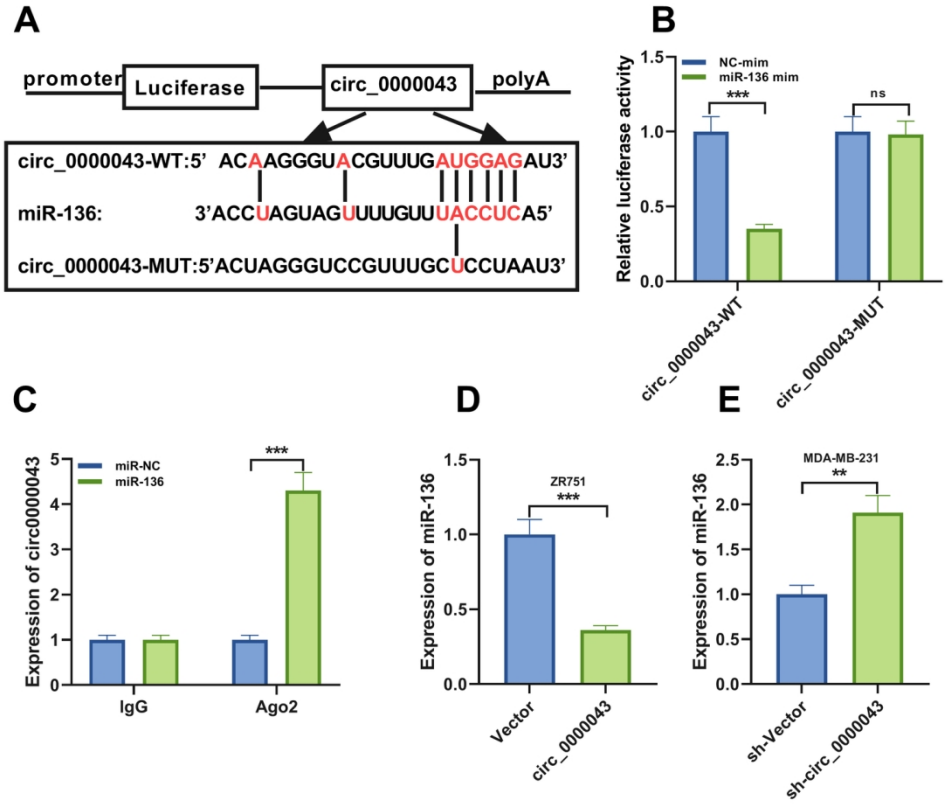

Figure 3: Circ_0000043 had a targeting relationship with miR-136.
A: Circ_0000043 contained a potential binding site for miR-136. B: The targeting relationship between circ 0000043 and miR-136 was validated by dual luciferase report assay with MDA-MB-231 cells. C: In MDA-MB-231 cells, RIP experiment found that circ_0000043 directly interacted with miR-136. D-E: qRT-PCR demonstrated that overexpression of circ_0000043 in ZR751 cells inhibited miR-136 expression and knockdown of circ_0000043 in MDA-MB-231 cells promoted miR-136 expression.
P > 0.05 denoted by ns, P < 0.01 denoted by **, P < 0.001 denoted by ***.

135x118mm (300 x 300 DPI)

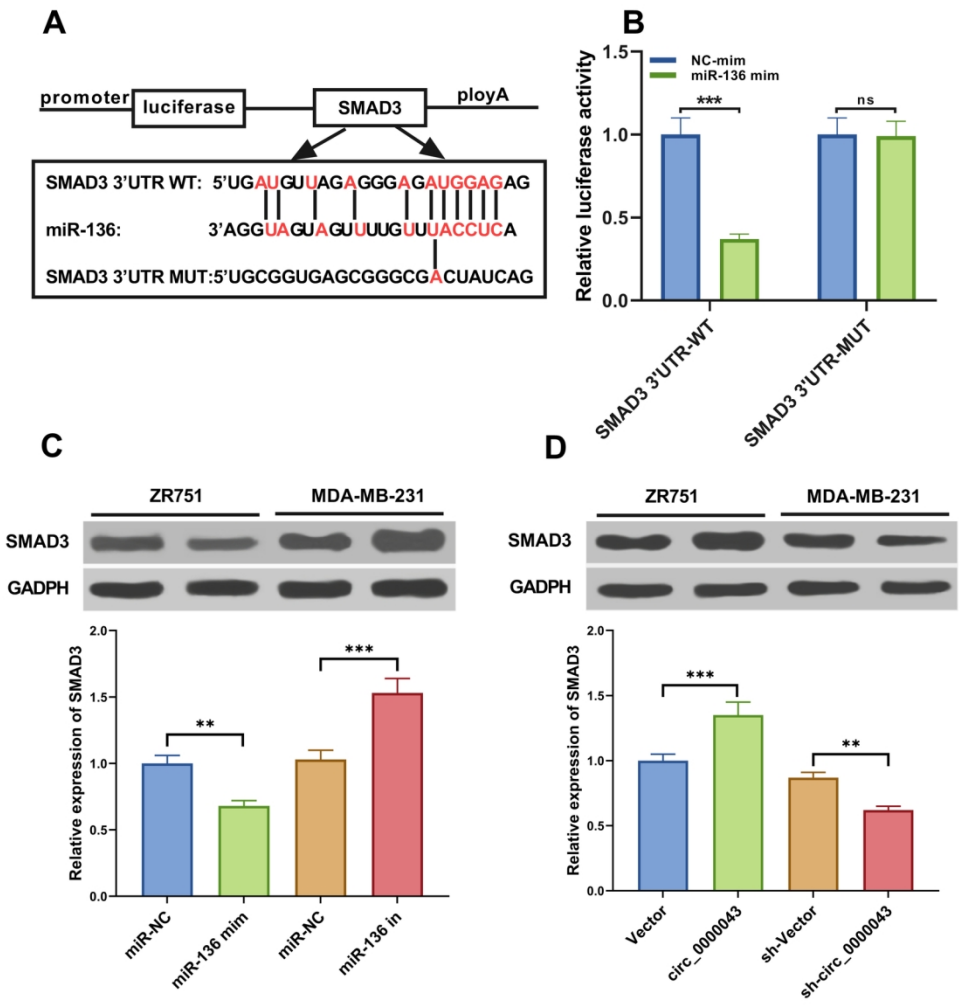

Figure 4: Smad3 was a downstream target of miR-136.
A: The 3'UTR of Smad3 was found to contain a potential binding site for miR-136. B: Dual luciferase report assay was used to detect the targeting relationship between miR-136 and Smad3 in MDA-MB-231 cells. C-D: Western blot assay data showed that miR-136 inhibited SMAD3 expression but circ_0000043 promoted SMAD3 expression.
P > 0.05 denoted by ns, P < 0.01 denoted by **, P < 0.001 denoted by *** .

150x154mm (300 x 300 DPI)

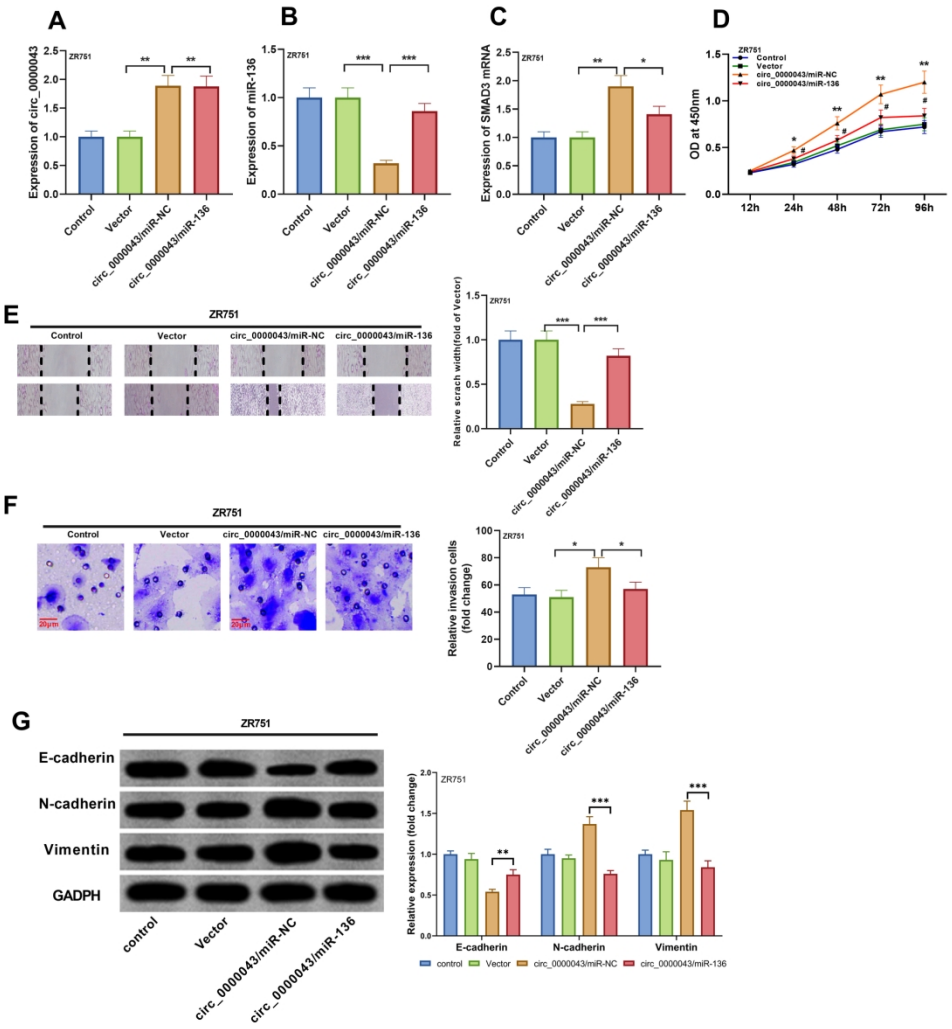

Figure 5: Circ_0000043 promoted BC cell proliferation, metastasis, and EMT through miR-136 / Smad3 axis. A-C: After miR-136 mimics were transfected into ZR751 cells overexpressing circ_0000043, the expressions of circ_0000043, miR-136 and Smad3 mRNA were detected by RT-PCR. D: CCK-8 assay indicated that miR-136 reversed the effect of circ_0000043 on proliferation of ZR751 cells. E-F: Wound healing and Transwell assays suggested that miR-136 reversed the effects of circ_0000043 on migration and invasion of ZR751 cells. G: Western blot assay demonstrated that miR-136 reversed the effect of circ_0000043 on EMT of ZR751 cells.

P <0.05 indicated by *, P < 0.01 indicated by **, P < 0.001 indicated by ***. In figure D, , P <0.05 indicated by *, P < 0.01 indicated by ** (vs Vector group); P < 0.05 indicated by # (vs circ_0000043 / miR-NC group)

193x202mm (300 x 300 DPI)

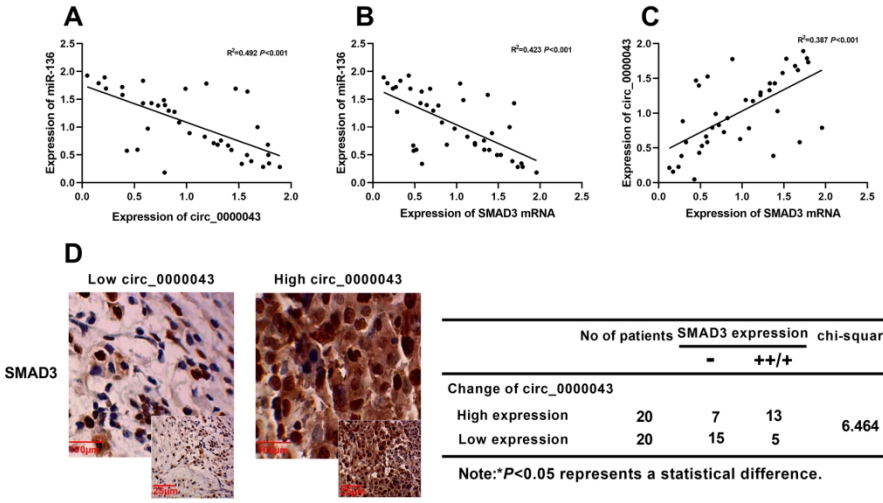

	No of patients	SMAD3 expression		chi-square value	*P* value
		-	++/+		
Change of circ_0000043					
High expression	20	7	13	6.464	0.011*
Low expression	20	15	5		

Note:*$P<0.05$ represents a statistical difference.

Figure 6: The correlation of circ_0000043, Smad3 and miR-136 in BC tissues.
A-C: The negative correlations between miR-136 and circ_0000043, miR-135 and SMAD3 mRNA, and the positive correlation between circ_0000043 and SMAD3 mRNA in BC tissues were found by Pearson's correlation analysis. D: Immunohistochemical staining was performed, and chi-square test indicated the significant positive correlation between Smad3 protein expression and circ_0000043 expression in BC samples.

182x97mm (300 x 300 DPI)